



# La-based bulk metallic glass failure analysis under static and dynamic loading



Jun Liu\*, V.P.W. Shim

Impact Mechanics Laboratory, Department of Mechanical Engineering, National University of Singapore, 10 Kent Ridge Crescent, Singapore 119260, Singapore

## ARTICLE INFO

### Article history:

Received 9 January 2013  
Received in revised form  
8 April 2013  
Accepted 13 April 2013  
Available online 23 April 2013

### Keywords:

Bulk metallic glass  
Shear band  
Split-Hopkinson Pressure Bar (SHPB)  
Modelling of temperature evolution  
Strain rate effects

## ABSTRACT

Samples of La-based bulk metallic glass were tested under both static and dynamic compression, and their failure analysed. The strain rates imposed ranged from  $10^{-4}$ /s to  $10^3$ /s. Quasi-static compression was performed using an Instron universal testing machine and dynamic compression was applied by means of a Split-Hopkinson Pressure Bar (SHPB). This study focuses on: (1) Shear band characteristics under static and dynamic compression. A high-speed optical camera was used to capture visual images of shear band initiation; fracture surfaces were also examined by SEM; (2) Modelling of shear band temperature evolution within the specimen, with the aid of high-speed infrared camera images, to capture the temperature profile of the shear bands; (3) Effect of strain rate on response of La-based BMG. It is postulated that the negative strain rate dependence observed arises from the non-uniform direction of stress within the material, and stress concentration inside specimens.

© 2013 Elsevier Ltd. All rights reserved.

## 1. Introduction

Bulk metallic glasses (BMGs) have attracted increasing attention in recent years because of their high strengths and hardness. However, because of the lack of post-yield hardening, plastic deformation in BMG generally concentrates within an extremely thin shear band ( $\sim 20$  nm) [1], which leads to rapid catastrophic failure, limiting the application of BMG in actual structures. This characteristic has motivated extensive study into the nature of such shear bands and the failure mechanisms of BMG. However, because of limitations in experimental techniques, the precise nature of BMG failure remains unclear. Furthermore, recent experimental results [2–14] indicate that different classes of BMGs possess different failure mechanisms and fracture behaviour. This motivates further experimentation to obtain a better understanding of the deformation mechanisms in BMG material.

In this study, various experimental techniques are combined, and hierarchical multi-scale modelling of heat conduction is undertaken to examine the failure of La-based amorphous alloys. This includes the effect of strain rate, temperature distribution profile and shear band characteristics. To date, there appears to be no published information on shear band temperature characterisation

and dynamic constitutive behaviour of this class of BMGs. The present investigation contributes to a better understanding of deformation in this type of material, and could serve as a guide for future development of La-based BMG composites.

## 2. Material fabrication and testing

Monolithic  $\text{La}_{62}\text{Al}_{14}\text{Cu}_{12}\text{Ni}_{12}$  amorphous alloy was prepared by arc-melting a mixture of La (99.9%), Al (99.9%), Ni (99.98%) and Cu (99.9999%) in an argon atmosphere. The molten alloy was then injected into a copper mould to produce ingots. The as-cast ingots were machined into small cylindrical specimens of 4 mm diameter. Samples with two aspect ratios were fabricated, 1:1 and 2:1, for both static and dynamic compression tests, to ascertain whether there is a size effect. The amorphous nature of the microstructure was examined by X-ray Diffraction (XRD).

Compression tests at quasi-static strain rates were performed using an Instron 8874 universal testing machine. The specimen contact surfaces were lubricated using molybdenum disulphide ( $\text{MoS}_2$ ) to reduce friction, and the strain rates ranged from  $5 \times 10^{-4}$ /s to  $5 \times 10^{-2}$ /s, which were obtained from strain gauges mounted on the specimens. Dynamic compression tests were conducted using a Split-Hopkinson Pressure Bar (SHPB) device. Since the material is brittle and fails at small strains, pulse shaping was used to enhance the reliability of results. Annealed copper disks were employed as pulse shapers, and inserted between the striker and

\* Corresponding author. Tel.: +65 92268572.

E-mail addresses: [liujun@nus.edu.sg](mailto:liujun@nus.edu.sg), [nickliujun@gmail.com](mailto:nickliujun@gmail.com) (J. Liu).

the input bar to promote stress equilibrium and a constant strain rate before fracture occurs. The brittle nature of the material results in early catastrophic failure (around  $15 \mu\text{s} \sim 25 \mu\text{s}$  after loading), which limits the strain rate that can be imposed. In the tests, the strain rates ranged from 600/s to 1500/s. High-speed optical and infrared (IR) cameras were used to capture features of the shear bands at fracture. The fracture surfaces were observed using field emission scanning electron microscopy (FE-SEM).

### 3. Analysis of results

#### 3.1. Shear band characteristics

Fig. 1 shows a typical quasi-static compressive stress–strain curve for  $\text{La}_{62}\text{Al}_{14}\text{Cu}_{12}\text{Ni}_{12}$  BMG alloy. It indicates that there is essentially no plastic response, and the sample fails by catastrophic fracture. To investigate the failure process in more detail, an optical high-speed camera was used to capture images of the shear band for static and dynamic compression, as shown in Figs. 2 and 3 (the time intervals between the images are approximately  $7 \mu\text{s}$  and  $4 \mu\text{s}$ , respectively). The instants the images correspond to are indicated, and  $t_0$  is a reference time. These show clearly how the shear bands initiate and propagate to the point of fracture; the process is accompanied by the emission of sparks, indicating a large temperature increase within the shear band, and the entire duration spans just tens of microseconds. It is noted that the fracture patterns for static and dynamic loading differ. Under quasi-static loading, only one major shear band is evident. However, for dynamic loading, catastrophic failure occurs by fracture of the sample into several fragments. Fig. 4 illustrates the fracture of different samples under dynamic compression, and shows that this fragmentation response is consistent – i.e. multiple shear bands are generated instead of only one in static loading.

Fig. 5 shows SEM images of different regions on a fracture surface of a sample after static compression. The vein pattern morphologies indicate micro-plasticity at fracture, while the U-shaped dimples (indicated by the white arrows) reveal the direction of plastic flow, which corresponds to the black arrows in the figure. How the shear band propagates and how the heat generated influences plastic flow can be clearly seen. The total fracture surface can be divided into three regions, and the location of these areas on the fracture surface, as well as the flow direction, are shown in Fig. 5(a). Fig. 5(b) displays a regular strip-like vein pattern, which defines the commencement of shear band initiation, when heating at this location is not obvious. Fig. 5(c) corresponds to an area where the heat generated by plastic deformation has accumulated within the shear band and become significant; there is a clear transition from a regular strip-pattern to large irregular dimples. In Fig. 5(d), heating within the shear band is

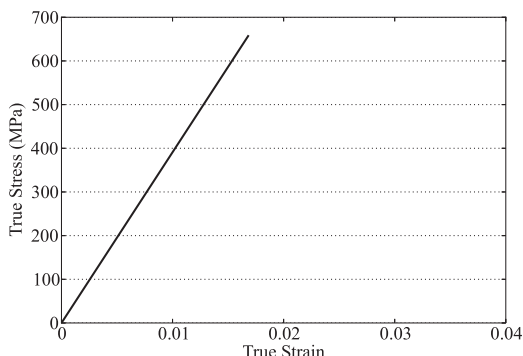


Fig. 1. The true stress–strain curve for static compression.

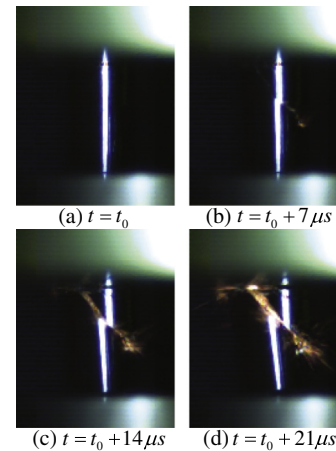


Fig. 2. Optical images of shear band evolution for static compression.

significant and affects the deformation; hence, the plastic flow is quite different from that in region (b). The large dimples and molten droplets indicate that heating in this region is substantial and has altered the material behaviour during shear band propagation. However, although the dimple pattern is irregular, the dimple direction is still consistent, and the flow direction can be identified via the U-shaped profiles.

Fig. 6 shows SEM images of a fracture surface after dynamic compression. Although it also has a dimple-like morphology like the fracture surface for static compression, the details are quite different. Fig. 6(a) shows a localised area of the fracture surface, and the arrows identify the strip pattern directions. Fig. 6(b) is a magnification of area (b) in Fig. 6(a); the arrows indicate the direction of the U-shape dimples. They show that these U-shape dimples no longer align with the direction of the strip pattern. Furthermore, Fig. 6(c) and the magnification of area (d) in Fig. 6(d) show that it is almost impossible to identify the flow direction through the dimple structure. From Figs. 5 and 6, it can be seen that the vein-pattern for a statically-compressed sample has a more uniform direction compared with the dynamically-compressed sample, which indicates that the stress distribution inside the dynamically-loaded sample is more complex and heterogeneous.

#### 3.2. Heat evolution in shear band

Earlier researchers assumed that the highly localised catastrophic fracture in BMG comes from local adiabatic heating [15], similar to what happens in crystalline materials [16]. However, with the development of BMG micro-mechanism deformation theory, there is a growing conclusion that nano-level structural instability, caused by the initiation of free volume [17] and

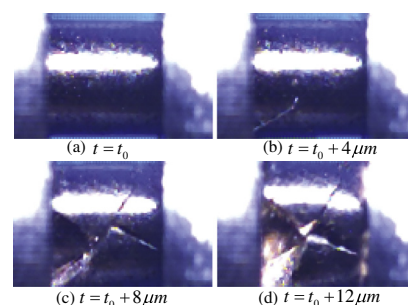


Fig. 3. Optical images of shear band evolution for dynamic compression.

Download English Version:

<https://daneshyari.com/en/article/7173270>

Download Persian Version:

<https://daneshyari.com/article/7173270>

[Daneshyari.com](https://daneshyari.com)